Journal of Applied Mechanics and Technical Physics, Vol. 44, No. 6, pp. 858–865, 2003

CALCULATION OF HEAVY GAS SPREADING OVER THE EARTH SURFACE BY A THREE-DIMENSIONAL MODEL

I. M. Bayanov,[1] M. Z. Gil'mullin,[1] and V. Sh. Shagapov[2]

UDC 539.532.551.575

A mathematical model is constructed for motion of a heavy gas along the underlying terrain on the basis of equations of gas dynamics with allowance for the force of gravity, transfer by air masses, and turbulent diffusion. With the use of the method of coarse particles, the time dependences of the coordinates of the fore front, upper boundary, and volume of the cloud of a heavy gas in the presence and absence of wind are analyzed. It is shown that turbulent diffusion leads to a linear increase in cloud volume in time. Three-dimensional shapes of the heavy gas cloud are obtained for various ambient conditions. It is shown that, despite diffusion, the heavy gas spreads predominantly along the underlying terrain.

Key words: *transfer of admixtures, turbulent diffusion, three-dimensional model, method of coarse particles.*

Introduction. Significant amounts of industrial wastes into the surface zone of the atmospheric boundary layer are responsible for the arduous ecological situation in many regions. Such wastes are hazardous for nature and mankind, since they propagate along the underlying terrain. The description of this phenomenon requires a detailed study of the mechanism of this process and development of models of transfer of admixtures in the ambient space.

Industrial wastes are mixtures of gases, vapors, aerosols, and solid particles; propagation of these substances is studied on the basis of rather complicated mathematical models [1].

The characteristics of the heavy gas (mixture of wastes with atmospheric air) are determined by the Richardson number [2]

$$\mathrm{Ri} = (\rho - \rho_\mathrm{a})gh/(\rho_\mathrm{a}v^2),$$

which is the ratio of the acceleration of gravity of a turbulent particle $(\rho - \rho_\mathrm{a})g/\rho_\mathrm{a}$ to inertial acceleration v^2/h caused by turbulent fluctuations of air with a velocity of the order of dynamic velocity u within a cloud of size h.

The Richardson criterion $\mathrm{Ri} > 10$ imposes a condition on the mean density of the mixture of the heavy gas and atmospheric air ρ in the form

$$(\rho - \rho_\mathrm{a})/\rho_\mathrm{a} > 0.004 \tag{1}$$

if we assume that the characteristic dynamic velocity for the neutral state of the atmosphere is $v = 0.2$ m/sec and the cloud size is $h = 10$ m [2].

In what follows, the heavy gas is understood as a mixture of air with a gas whose molar weight μ_g (this gas will be called the heavy component) is greater than the mean molar weight of air μ_a ($\mu_\mathrm{g} > \mu_\mathrm{a}$).

1. Mathematical Model. The motion of the heavy gas is described by the Euler equations and diffusion equations [3–5]. Allowance for a large number of factors determining gas motion requires large computer resources; therefore, complicated models are usually calculated in a two-dimensional formulation [3]. A three-dimensional

[1]Birsk State Pedagogical Institute, Birsk 452450. [2]Institute of Mechanics at the Ufa Scientific Center, Russian Academy of Sciences, Ufa 450000. Translated from Prikladnaya Mekhanika i Tekhnicheskaya Fizika, Vol. 44, No. 6, pp. 130–139, November–December, 2003. Original article submitted March 31, 2003; revision submitted May 12, 2003.

 0021-8944/03/4406-0858 $25.00

problem of spreading of a heavy gas in a spatial region of size 100–1000 m can be solved within the framework of a simplified model.

In our opinion, in most cases, the laws of propagation of heavy wastes in the atmosphere mainly depend on the action of the force of gravity, transfer by air masses (wind), and diffusion determined by small-scale turbulent fluctuations of wind velocity.

The present model describes the motion of air masses in the surface atmospheric layer up to 100 m thick, where the characteristics of vertical air flows remain almost unchanged with height [1]. Therefore, equilibrium stratification is observed if the temperature has a weak dependence on height.

We write the Euler equations with allowance for the force of gravity:

$$\frac{\partial \rho}{\partial t} + \operatorname{div}(\rho \boldsymbol{v}) = 0,$$
$$\frac{\partial (\rho \boldsymbol{v})}{\partial t} + \operatorname{div}(\rho(\boldsymbol{v}, \nabla)\boldsymbol{v}) + \operatorname{grad} p = -\rho \boldsymbol{g}. \tag{2}$$

Here $\boldsymbol{v}$ is the velocity of the mixture, p is the pressure in the mixture, $\boldsymbol{g}$ is the acceleration of gravity, and t is the time.

The dependence of pressure on density and concentration of the heavy component is written in the form of the Clapeyron–Mendeleev equation with allowance for Dalton's law:

$$p = \rho R T \Big(\frac{C}{\mu_{\mathrm{g}}} + \frac{1 - C}{\mu_{\mathrm{a}}} \Big). \tag{3}$$

Here R is the universal gas constant, T is the temperature of the mixture, which is assumed to be constant, and C is the mass concentration of the heavy component.

To take into account active mixing of the heavy component with the atmosphere, we have to write the diffusion equation derived from the continuity equation within the framework of the K-model of turbulent diffusion [6, 7]:

$$\frac{\partial (\rho C)}{\partial t} + \operatorname{div}(\rho C \boldsymbol{v}) = \frac{\partial}{\partial x}\Big(k_x \rho \frac{\partial C}{\partial x} \Big) + \frac{\partial}{\partial y}\Big(k_y \rho \frac{\partial C}{\partial y} \Big) + \frac{\partial}{\partial z}\Big(k_z \rho \frac{\partial C}{\partial z} \Big). \tag{4}$$

In the case of equilibrium stratification, the coefficients of turbulent diffusion depend on height. Moreover, the coefficients of horizontal and vertical diffusion differ in value and character of their dependence on height z and are usually written in the following form [1]:

$$k_x = k_y = k_0 u_1 \log(z/z_0)/\log(z_1/z_0), \qquad k_z = k_1 z/z_1.$$

Here k_0 is a proportionality coefficient, u_1 is an empirical parameter, z_0 is the roughness coefficient of the underlying terrain, and k_1 is the coefficient of vertical turbulent diffusion at the height z_1 (z_1 is the scale height). This distribution of turbulent diffusion coefficients is valid for the surface atmospheric layer ($z \leqslant 100$ m).

Thus, system (2)–(4) that describes gas motion includes the continuity equation, the Euler equations, the equation of turbulent diffusion, and the equation of state for the heavy gas and atmosphere.

2. Numerical Model. The numerical model is based on solving system (2)–(4) by the method of coarse particles [8], which is one of the methods of splitting of the initial unsteady system of gas-dynamic equations written in the form of conservation laws in terms of physical processes.

The computational domain is divided by the computational grid into $N = N_x N_y N_z$ cells, which are the so-called coarse particles. At the first stage, the grid moves together with the substance, and there are no mass fluxes through cell boundaries. The coarse particles move due to a pressure gradient. The substance density remains unchanged. At this stage, intermediate values of velocity and concentration are calculated:

$$\tilde{v}^n_{x\,i,j,k} = v^n_{x\,i,j,k} - \frac{p^n_{i+1,j,k} - p^n_{i-1,j,k}}{\Delta x_i + \Delta x_{i-1}} \frac{\Delta t}{\rho^n_{i,j,k}}, \qquad \tilde{v}^n_{y\,i,j,k} = v^n_{y\,i,j,k} - \frac{p^n_{i,j+1,k} - p^n_{i,j-1,k}}{\Delta y_j + \Delta y_{j-1}} \frac{\Delta t}{\rho^n_{i,j,k}},$$

$$\tilde{v}^n_{z\,i,j,k} = v^n_{z\,i,j,k} - \frac{p^n_{i,j,k+1} - p^n_{i,j,k-1}}{\Delta z_k + \Delta z_{k-1}} \frac{\Delta t}{\rho^n_{i,j,k}} - g\Delta t,$$

$$\tilde{C}^n_{i,j,k} = C^n_{i,j,k} + A \frac{\Delta t}{\rho^n_{i,j,k}}, \qquad A = A_1 + A_2 + A_3,$$

$$A_1 = k_0 u_1 \frac{\log(z_k/z_0)}{\log(z_1/z_0)} \Big(\rho^n_{i+1,j,k} \frac{2(C^n_{i+1,j,k} - C^n_{i,j,k})}{\Delta x_i + \Delta x_{i+1}} - \rho^n_{i-1,j,k} \frac{2(C^n_{i,j,k} - C^n_{i-1,j,k})}{\Delta x_{i-1} + \Delta x_i} \Big) \frac{3}{\Delta x_{i-1} + \Delta x_i + \Delta x_{i+1}},$$

$$A_2 = k_0 u_1 \frac{\log(z_k/z_0)}{\log(z_1/z_0)} \Big(\rho^n_{i,j+1,k} \frac{2(C^n_{i,j+1,k} - C^n_{i,j,k})}{\Delta y_j + \Delta y_{j+1}} - \rho^n_{i,j-1,k} \frac{2(C^n_{i,j,k} - C^n_{i,j-1,k})}{\Delta y_{j-1} + \Delta y_j} \Big) \quad \frac{3}{\Delta y_{j-1} + \Delta y_j + \Delta y_{j+1}},$$

$$A_3 = \frac{k_1}{z_1} \Big(\rho^n_{i,j,k+1} z_{k+1} \frac{2(C^n_{i,j,k+1} - C^n_{i,j,k})}{\Delta z_k + \Delta z_{k+1}} - \rho^n_{i,j,k-1} z_{k-1} \frac{2(C^n_{i,j,k} - C^n_{i,j,k-1})}{\Delta z_{k-1} + \Delta z_k} \Big) \frac{3}{\Delta z_{k-1} + \Delta z_k + \Delta z_{k+1}}.$$

At the second stage, the computational grid returns to the initial state, and mass fluxes ΔM through cell boundaries are calculated using intermediate values of velocity. The values of ΔM are calculated by the first-order formulas:

$$\Delta M^n_{i+1/2,j,k} = \begin{cases} \rho^n_{i,j,k} (\tilde v^n_{x\,i,j,k} + \tilde v^n_{x\,i+1,j,k})\, \Delta y_j\, \Delta z_k\, \Delta t/2, & \tilde v^n_{x\,i,j,k} + \tilde v^n_{x\,i+1,j,k} > 0, \\ \rho^n_{i+1,j,k} (\tilde v^n_{x\,i,j,k} + \tilde v^n_{x\,i+1,j,k})\, \Delta y_j\, \Delta z_k\, \Delta t/2, & \tilde v^n_{x\,i,j,k} + \tilde v^n_{x\,i+1,j,k} < 0. \end{cases}$$

The values of $\Delta M^n_{i-1/2,j,k}$ are calculated in a similar manner. In this work, we use the method of fluxes [9]; therefore, the fluxes of momentum $\Delta(Mv)$ and concentration ΔC, which "move" together with the mass flux, are also calculated. For example, the momentum and concentration fluxes through the right boundary of the cell along the x axis are written in the form

$$\Delta(Mv)^n_{i+1/2,j,k} = \Delta M^n_{i+1/2,j,k} \tilde v^n_{x\,i,j,k}, \qquad \Delta C^n_{i+1/2,j,k} = \Delta M^n_{i+1/2,j,k} \tilde C^n_{i,j,k}.$$

At the third stage, we calculate the final values of density, velocity, and concentration at the next time step with allowance for fluxes of mass, momentum, and concentration [$X = X(v_x, v_y, v_z, C)$]:

$$X^{n+1}_{i,j,k} = \frac{\rho^n_{i,j,k}}{\rho^{n+1}_{i,j,k}} \tilde X^n_{i,j,k} + \frac{1}{\rho^{n+1}_{i,j,k}\, \Delta x_i\, \Delta y_j\, \Delta z_k} \Big(\tilde X^n_{i-1,j,k}\, \Delta M^n_{i-1/2,j,k} + \tilde X^n_{i,j-1,k}\, \Delta M^n_{i,j-1/2,k}$$

$$+ \tilde X^n_{i,j,k-1}\, \Delta M^n_{i,j,k-1/2} - \tilde X^n_{i+1,j,k}\, \Delta M^n_{i+1/2,j,k} - \tilde X^n_{i,j+1,k}\, \Delta M^n_{i,j+1/2,k} - \tilde X^n_{i,j,k+1}\, \Delta M^n_{i,j,k+1/2} \Big).$$

Then, from the equation of state, we find the pressure at the next time step

$$p^{n+1}_{i,j,k} = \rho^{n+1}_{i,j,k} RT (C^{n+1}_{i,j,k}/\mu_{\rm g} + (1 - C^{n+1}_{i,j,k})/\mu_{\rm a}).$$

After that, the calculation procedure is repeated.

Approximation of gas-dynamic equations by a numerical scheme of the method of coarse particles was performed by Belotserkovskii and Davydov in [8]. The order of approximation of the difference scheme of the method of coarse particles used equals unity within the entire computational domain both at internal points and at the boundaries.

The stability of this numerical scheme was also considered in [8]. An analysis of the system of difference equations shows that the scheme is stable at all stages if first-order formulas are used to calculate the mass fluxes ΔM. The time step is determined from the Courant condition $\Delta t = A\, \Delta x/c$, where c is the velocity of sound in the atmosphere and $A = \text{const} < 0.5$ is the safety factor [10].

An advantage of this numerical model is the stability of the scheme in the case of discontinuous solutions (e.g., jumplike distribution of the gas density at the initial time) and the applicability of the model within a wide range of velocities.

The model can be supplemented by the law of conservation of energy to allow for thermal effects (heat transfer, thermal diffusion, phase transitions, etc.). In the present work, the temperature distribution is constant within the entire computational domain.

3. Initial Conditions. The computational domain is a parallelepiped Ω in a coordinate system xyz. The initial size of the gas column Ω_1 is $x_1 \leqslant x \leqslant x_2$, $y_1 \leqslant y \leqslant y_2$, $z \leqslant z_1$. The initial pressure equals the atmospheric value:

$$p_0(x, y, z) = p_0 = p_{\rm a}.$$

The atmospheric pressure is determined by the barometric formula

$$p_{\rm a} = p_{\rm a0}\, {\rm e}^{-\mu_{\rm a} g z/(RT)}.$$

At the initial time, the region Ω_1 contains a pure gas with a molar weight $\mu_g > \mu_a$; hence, for $p = p_a$, the density of the heavy gas in the column is greater than the atmospheric density: $\rho = \rho_g > \rho_a$. The initial concentration of the heavy gas is

$$C = \begin{cases} 1, & (x, y, z) \in \Omega_1, \\ 0, & (x, y, z) \notin \Omega_1. \end{cases}$$

The initial gas velocity within the entire computational domain can be set depending on the wind velocity profile. In particular, if there is no wind, we have $\boldsymbol{v}(x, y, z) = 0$.

4. Boundary Conditions. For the numerical scheme to be identical at all points of the computational grid, additional ghost cells are introduced along all boundaries; the values of the sought quantities from the neighboring cells are repeated in the ghost cells. There are two types of boundaries: solid wall and open boundary. In the first case, the normal-to-wall velocity component changes its sign in the layer of ghost cells, and the remaining parameters of the gas are unchanged. In the second case, all components of velocity are transferred to the ghost cells without changes.

The external boundaries of the computational domain should be chosen rather far from the computational point for perturbations of gas parameters within the time period considered not to reach the boundaries. This condition together with the constraints on the coordinate step Δ increases the number of points N on each coordinate axis and, hence, the computation time in the three-dimensional case proportionally to N^3. To avoid this, nonuniform grids are used [11]. In the present work, we use a computational grid where the central region is uniform and the cell size linearly increases with distance from the center, beginning from a certain cell number. For instance, the cell size along the z axis is

$$\Delta z_k = \begin{cases} \Delta z_0, & k < N_{z0}, \\ (Ak + B)\Delta z_0, & k \geqslant N_{z0}. \end{cases}$$

In the uniform part of the grid, at the initial stage of heavy gas propagation, the gradients of flow parameters are rather high, and a fairly small spatial step Δ is required for several points of the grid to be located on the front of the cloud. As the gas cloud is expanding due to diffusion, the profiles of parameters are smoothed, and the step Δ can be increased.

5. Artificial Viscosity. The numerical scheme of the method of coarse particles is stable as a whole. At the first stage, however, there can appear instabilities caused by discontinuous solutions. Therefore, it is necessary to introduce a dissipative process that allows smoothing of the discontinuity front. In the present work, artificial viscosity (pseudoviscosity) is introduced at the first stage as an additional viscous pressure $p + q$ in the form [8]

$$q = \begin{cases} -\mu_0 \rho \, dv/dx, & dv/dx < 0, \\ 0, & dv/dx \geqslant 0, \end{cases}$$

where μ_0 is the viscosity.

Since the difference equations involve pressure, one has to take into account six values of q at the cell boundaries in the three-dimensional case:

$$q_{i+1,j,k} = \mu \, \frac{\rho^n_{i+1,j,k} \rho^n_{i,j,k}}{\rho^n_{i+1,j,k} + \rho^n_{i,j,k}} \, \frac{\tilde{v}^n_{i+1,j,k} + \tilde{v}^n_{i,j,k}}{\Delta x_i}.$$

In the absence of pseudoviscosity, the velocity profile has random spikes, which are accumulated during computations in the form of a constant component. Artificial viscosity smoothes the velocity profile.

6. Computation Results. We consider a hypothetical gas with a molar weight $\mu = 100$ g/mole as a heavy gas.

We composed a program that allows us to calculate the spatial distribution of the heavy gas at each time instant. To control the computation accuracy, the mass of the heavy gas is calculated at each time step by integration over the entire computational domain. The mass of the heavy gas is retained constant within 1% during the entire computation time, which is caused by the error of numerical differentiation of the concentration C with respect to coordinates in the diffusion equation. The main contribution to the error is made at the first ten time steps, when the profile of C at the cloud boundary is close to the stepwise shape.

In numerical experiments, we studied the influence of various factors (force of gravity, turbulent diffusion, and sidewind) on heavy gas propagation in two-dimensional (x, z) and three-dimensional (x, y, z) cases.

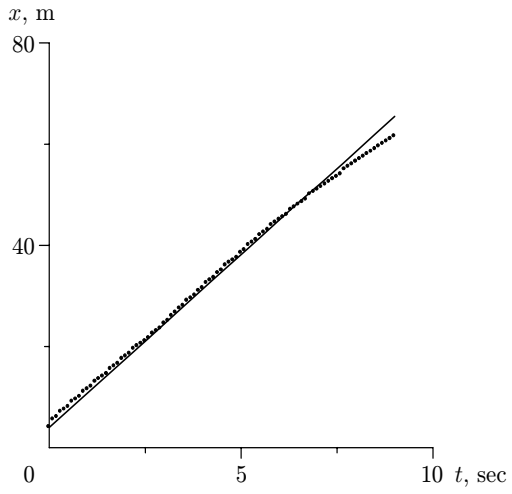

Fig. 1

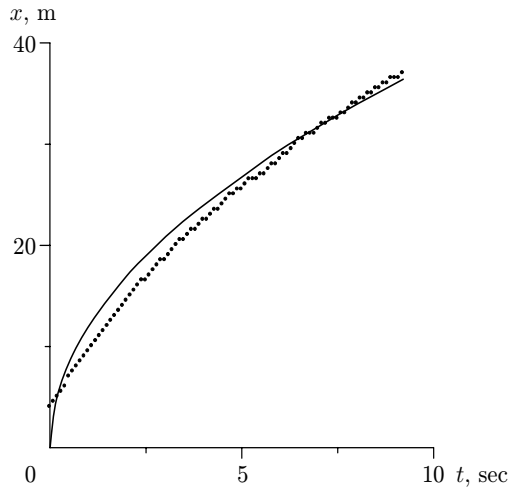

Fig. 2

Fig. 1. Coordinate of the front of the heavy gas cloud versus time in the two-dimensional case: the points show the calculated values and the curve is approximation by the linear dependence $x = a_x t + x_0$.

Fig. 2. Coordinate of the front of the heavy gas cloud versus time in the three-dimensional case: the points show the calculated values and the curve is approximation by the dependence $x = A\sqrt{t}$.

In the course of propagation of the heavy gas cloud, the concentration decreases due to turbulent diffusion and can reach the critical value $C_{\rm cr}$ where the heavy gas becomes a neutral one. For a gas with a molar weight $\mu = 100$ g/mole, we have $C_{\rm cr} = 5.6 \cdot 10^{-3}$ from condition (1). Therefore, the conventional boundary of the heavy gas cloud can be defined as a surface formed by a set of points with an identical concentration: $C = 0.01$.

The motion of the heavy gas is characterized by the following parameters registered at the cloud boundary: coordinate of the fore front $x_{\rm f}$ on the underlying terrain, maximum height $h_{\max}$, and effective volume of the cloud $V_{\rm g}$.

We consider the motion of the heavy gas in the absence of wind, i.e., with $\boldsymbol{v}(x, y, z, 0) = 0$ within the entire computational domain.

In the case of motion over two coordinates (x, z), the coordinate of the fore front depends linearly on time, which indicates a uniform motion of the gas (Fig. 1). This conclusion was made in [12]. In the case of motion over three coordinates (x, y, z), the velocity of the fore front decreases ($x_{\rm f} \sim \sqrt{t}$) because of the more rapid decrease in the concentration gradient (Fig. 2), since gas spreading in the horizontal direction proceeds over two coordinates (x, y).

The initial increase in cloud height in the center is associated with a higher initial gradient of concentration at the upper boundary of the cloud and, hence, with intense diffusion. In what follows, the cloud height decreases smoothly almost twofold, which is caused by smoothing of the concentration gradient and a decrease in vertical diffusion. In this case, the action of the force of gravity becomes more substantial (Fig. 3). The discreteness of the values of z in Fig. 3 is caused by the step of the computational grid $\Delta = 0.5$ m.

The increase in effective volume of the gas with time is determined by diffusion only and, hence, is proportional to the cloud surface area S. The linearity of the dependence $V(t)$ is caused by the character of the dependence of the cloud radius (in fact, the coordinate of the fore front $x_{\rm f}$) on time and a small decrease in height: $S \sim x_{\rm f}^2 \sim t$ (Fig. 4).

The distribution of the heavy gas concentration in the plane xz over the center of the cloud at the time $t = 5$ sec shows that the heavy gas, despite significant diffusion, spreads along the underlying terrain (Fig. 5). This is also evidenced by the shape of the cloud surface determined by the level $C = 0.01$ at the same time (Fig. 6).

We consider the influence of sidewind on gas motion. The presence of wind can be set in initial and boundary conditions: at the initial time $v_x(0, x, y, z) = f(z)$ and at one of the boundaries of the computational domain $v_x(t, 0, y, z) = f(z)$. The wind velocity profile in the surface zone is represented as the logarithmic dependence [1]

$$v = v_0 \ln (z/z_0 + 1).$$

The time dependences of the coordinate of the fore front on the underlying terrain in the presence and absence of wind are in qualitative agreement (Fig. 7).

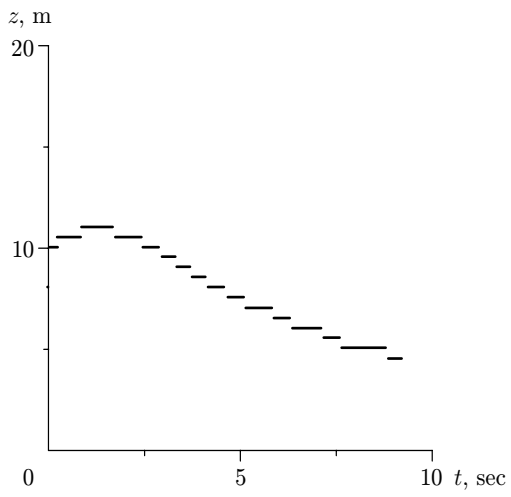

Fig. 3

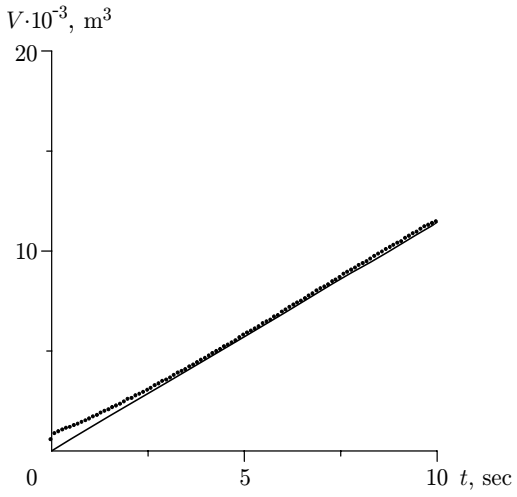

Fig. 4

Fig. 3. Height of the heavy gas cloud in the center versus time ($\Delta = 0.5$ m.)

Fig. 4. Volume of the heavy gas cloud versus time: the points show the calculated values and the curve is approximation by the dependence $V = a_V t + V_0$.

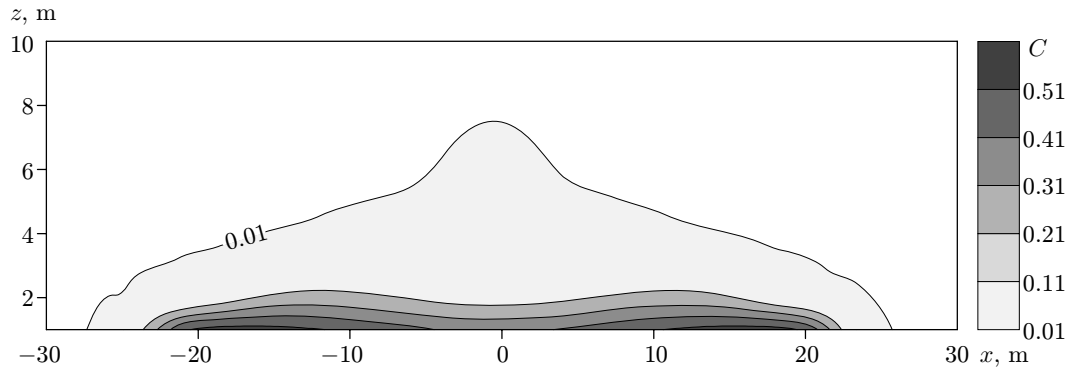

Fig. 5. Distribution of the heavy gas concentration in the plane $y = 0$ at $t = 5$ sec.

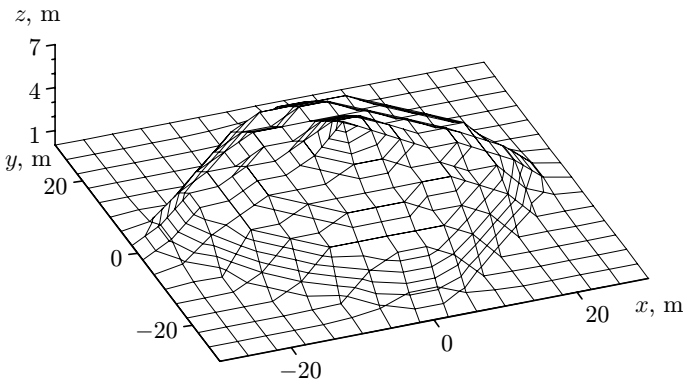

Fig. 6. Shape of the heavy gas cloud surface determined by the level of gas concentration $C = 0.01$ at $t = 5$ sec.

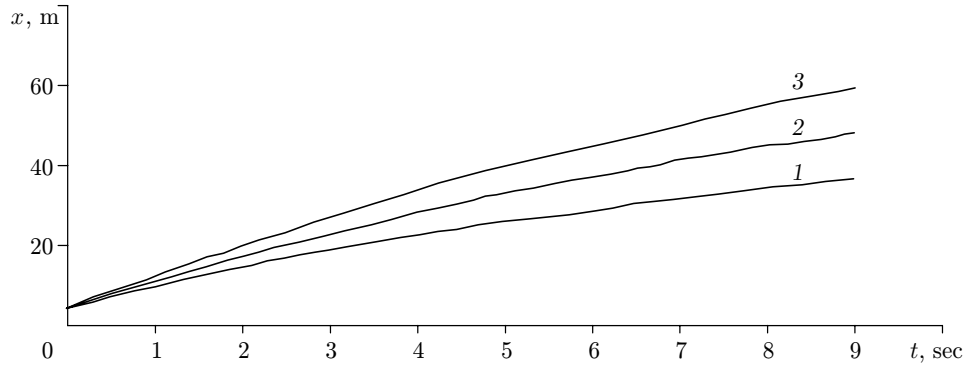

Fig. 7. Coordinate of the cloud front versus time for different sidewind velocities ($z_0 = 8$ m): $v_{0x} = 0$ (1), 2 (2), and 4 m/sec (3).

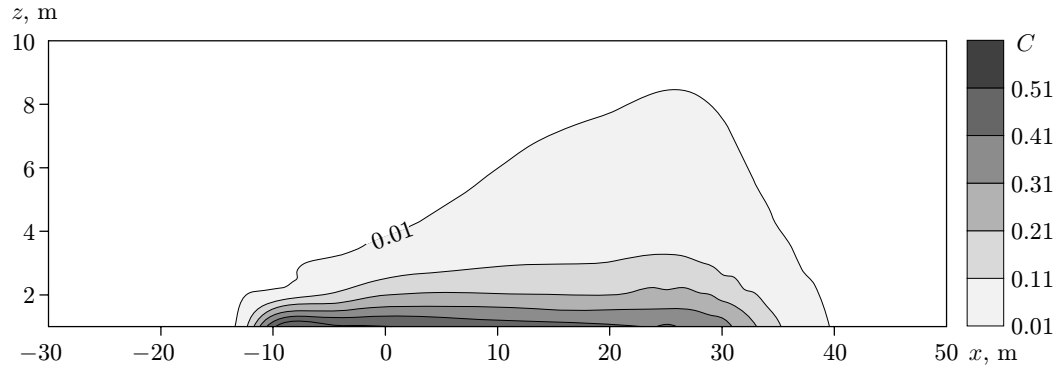

Fig. 8. Distribution of the heavy gas concentration in the plane $y = 0$ in the presence of wind ($t = 5$ sec, $z_0 = 8$ m, and $v_{0x} = 4$ m/sec).

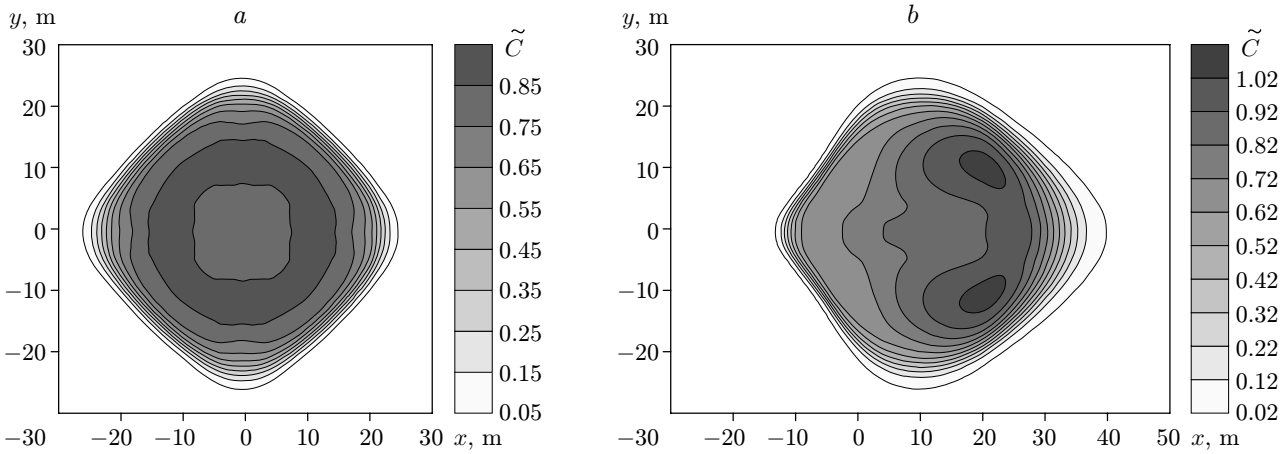

Fig. 9. Distribution of the gas concentration integrated over the height in the plane xy in the absence (a) and presence (b) of sidewind.

The presence of wind also changes the shape of the heavy gas cloud. The distribution of the heavy gas in the cloud in the plane xz is shown in Fig. 8, and the same distribution in the absence of wind is shown in Fig. 5. The heavy gas also spreads along the underlying terrain, but a significant shift of the cloud position is observed.

The distribution of the heavy gas in the plane xy (top view) can be obtained by integrating the gas concentration over the height z:

$$\tilde{C}(x, y, z, t) = \int_0^{z_{\max}} C(x, y, z, t)\, dz.$$

In the absence of wind (Fig. 9a), the distribution is symmetric. The circular wave of concentration propagates away from the cloud center. In the presence of wind (Fig. 9b), the cloud is shifted along the x axis. The character of motion along the y axis remains unchanged: two concentration waves diverging from the cloud center are observed.

7. Conclusions. The mathematical model proposed allows one to study the effect of the most important factors (force of gravity, turbulent diffusion, and wind) on the motion of a heavy gas in the atmosphere. The force of gravity prevents active mixing of the heavy gas with air, and the gas cloud spreads along the underlying terrain. The presence of wind shifts the cloud in the wind direction, but the motion of the heavy gas still has the character of spreading along the underlying terrain. This model can be supplemented by equations of thermal conductivity and phase transitions.

The numerical model proposed allows one to obtain the distribution of the heavy gas at each time step and to calculate the volume, height, and boundaries of the heavy gas cloud versus time. A linear character of the dependence of the cloud volume on time is revealed. This model allows one to calculate rapid motion of atmospheric wastes (explosion, jet, etc.).

REFERENCES

1. M. E. Berlyand, *Modern Problems of Atmospheric Diffusion and Contamination* [in Russian], Gidrometeoizdat, Leningrad (1975).
2. O. V. Dobrocheev, A. A. Kuleshov, and A. L. Lelakin, "A two dimensional model of heavy gas cloud dispersion under industrial accidents," Preprint No. IAE-5339/1, Kurchatov Inst. of Nuclear Energy, Moscow (1991).
3. R. N. Kuz'min, A. A. Kuleshov, N. P. Savenkova, and S. V. Filippova, "Modeling of accidents on an industrial enterprise with exhaustion of heavy gases and liquids," *Mat. Model.*, **10**, No. 8, 33–42 (1998).
4. V. V. Penenko and E. A. Tsvetova, "Some aspects of solving interrelated problems of ecology and climate," *J. Appl. Mech. Tech. Phys.*, **41**, No. 5, 907–914 (2000).
5. G. I. Marchuk, A. E. Aloyan, V. N. Piskunov, and V. D. Egorov, "Propagation of admixtures in the atmosphere with allowance for condensation," *Izv. Ross. Akad. Nauk, Fiz. Atmos. Okeana*, **32**, No. 5, 745–752 (1996).
6. J. A. Bussinger, "Basic notions and equations," in: Atmospheric Turbulence and Propagation of Admixtures: Lecture Course [in Russian], Gidrometeoizdat, Leningrad (1985), pp. 18–51.
7. V. V. Penenko and A. E. Aloyan, *Models and Methods for Environment Protection Problems* [in Russian], Nauka, Novosibirsk (1985).
8. O. M. Belotserkovskii and Yu. M. Davydov, *Method of Coarse Particles in Gas Dynamics* [in Russian], Nauka, Moscow (1982).
9. O. M. Belotserkovskii and L. I. Severinov, "Conservative method of 'fluxes' and calculation of a viscous heat-conducting gas flow around a finite-size body," *Zh. Vychisl. Mat. Mat. Fiz.*, **13**, No. 2, 385–397 (1973).
10. V. V. Ostapenko, "Numerical simulation of wave flows caused by a shoreside landslide," *J. Appl. Mech. Tech. Phys.*, **40**, No. 4, 647–654 (1999).
11. Yu. M. Davydov, "Structure of approximation viscosity," *Dokl. Akad. Nauk SSSR*, **245**, No. 4, 812–815 (1979).
12. V. Sh. Shagapov and G. R. Galiaskarova, "Theory of smog accumulation in still air," *Izv. Ross. Akad. Nauk, Fiz. Atmos. Okeana*, **38**, No. 1, 71–80 (2002).